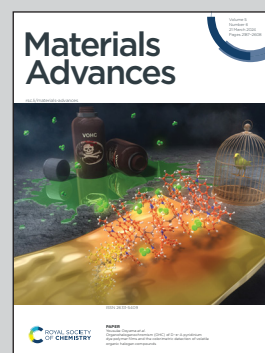**Showcasing research from Dr Yutaka Okazaki's research group, Graduate School of Energy Science, Kyoto University, Kyoto, Japan.**

Generation of time-multiplexed chiroptical information from multilayer-type luminescence-based circular polarization conversion films

Circularly polarized (CP) light generated from photoluminescence (PL) has great potential for the transmission of diverse forms of optical information including light intensity (brightness), spectral profile (color), and polarization (left-handed (LH)/right-handed (RH)), as well as temporal information corresponding to the PL lifetime of the CP light source. Here, we demonstrated a novel approach to time-multiplexing chiroptical information using multilayered luminescence-based CP convertors comprising two linearly polarized luminescence (LPL) films with different PL lifetimes and a quarter-wave retardation film.

ROYAL SOCIETY OF **CHEMISTRY**

rsc.li/materials-advances

PAPER

Check for updates

Generation of time-multiplexed chiroptical information from multilayer-type luminescence-based circular polarization conversion films†

Yutaka Okazaki, (iD) *[a] Hayaki Shimizu,[a] Kaito Nakamura,[a] Kyohei Yoshida, (iD) [b] Guillaume Raffy, (iD) [c] Misaki Kimura,[a] Keita Tsukamoto,[a] Rei Akasegawa,[a] Kan Hachiya, (iD) [a] Makoto Takafuji, (iD) [d] André Del Guerzo (iD) [c] and Takashi Sagawa (iD) *[a]

Circularly polarized (CP) light generated from photoluminescence (PL) has great potential for the transmission of diverse forms of optical information including light intensity (brightness), spectral profile (color), and polarization (left-handed (LH)/right-handed (RH)), as well as temporal information corresponding to the PL lifetime of the CP light source. However, a systematic approach to the design of CP light-generating materials for the conveyance of time-multiplexed chiroptical information has not yet been reported. Herein, we demonstrate a novel approach to time-multiplexing chiroptical information using multilayered luminescence-based CP convertors comprising two linearly polarized luminescence (LPL) films with different PL lifetimes and a quarter-wave retardation film. We prepared LPL films with short and long PL lifetimes by stretching films comprising poly[2-methoxy-5-(2-ethylhexyloxy)-1,4-phenylenevinylene] (MEH-PPV) and CdSe/CdS core/shell quantum rod (QR) luminogens, respectively. We then fabricated four types of multilayered luminescence-based CP convertors by laminating the LPL$_{MEH-PPV}$ and LPL$_{QR}$ films with quarter-wave retardation films, so that the azimuthal angles between the polarization axes of the LPL films and the fast axes of the quarter-wave films differed in each case. The resulting CP light comprised short- and long-lifetime components. Subsequently, we used a time-resolved spectroscopic technique to extract time-multiplexed chiroptical information from changes in the time-course of the spectral profile of the LH- and RH-CP light. The time-varying of CP light profiles were thereby read-out as time-multiplexed chiroptical information. Our findings will pave the way for the design of CP light-generating materials for conveying time-multiplexed chiroptical information.

Introduction

Polarized light has great potential for the delivery of information because it has variable characteristics such as intensity (brightness), wavelength (color), and polarization (linear and/or circular). In contrast to linearly polarized (LP) light, which conveys information according to the plane of propagation (vertical (v) or horizontal (h)), circularly polarized (CP) light conveys information according to the direction of rotation of the polarization plane (left-handed (LH) or right-handed (RH)). The rotational direction of the polarization plane is immutable, regardless of the angle between the sender and the receiver of optical information. Therefore, CP light is now considered potentially useful for various applications, such as anti-counterfeit printing and optical data storage.[1] In particular, CP light originating from photoluminescence (PL), including circularly polarized luminescence (CPL),[2] has the following distinctive advantages. First, optical information is concealed in visible light, whereas it is apparent in UV radiation. Second, the PL mechanism enables the multiplexing of optical information by the simple addition of other luminogens (summation of light), whereas the light absorption mechanism has a theoretical limitation with regard to the addition of other absorbers owing to a decrease in light intensity (subtraction of light). Third, the selection of luminogens with different PL lifetimes makes it theoretically possible to multiplex temporal information as an

[a] *Graduate School of Energy Science, Kyoto University, Yoshida-Honmachi, Sakyo-ku, Kyoto 606-8501, Japan. E-mail: okazaki.yutaka.8c@kyoto-u.ac.jp*

[b] *Materials Development Department, Kumamoto Industrial Research Institute, 3-11-38 Higashimachi, Higashi-ku, Kumamoto 862-0901, Japan*

[c] *Institut des Sciences Moléculaires (UMR5255 ISM), Université de Bordeaux – CNRS – Bordeaux INP, 351 Cours de la Libération, Talence 33405, France*

[d] *Department of Applied Chemistry and Biochemistry, Kumamoto University, 2-39-1 Kurokami, Chuo-ku, Kumamoto 860-8555, Japan*

† Electronic supplementary information (ESI) available: Experimental details and supplementary figures. See DOI: https://doi.org/10.1039/d3ma00648d
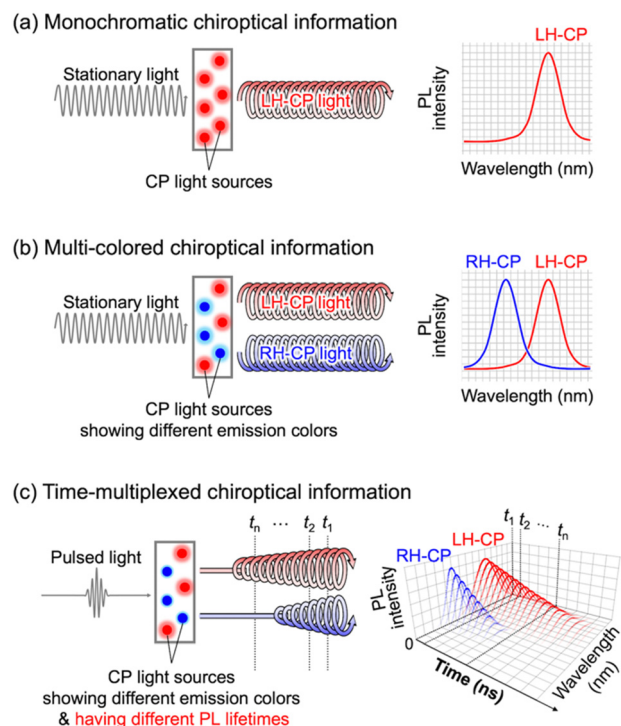
Fig. 1 Schematic illustration of (a) monochromatic and (b) multi-colored chiroptical information detected by steady-state PL spectroscopy, and (c) time-multiplexed chiroptical information detected by time-resolved PL spectroscopy.

Fig. 2 Schematic illustration of a multi-layered luminescence-based CP convertor for generating time-multiplexed chiroptical information.

additional parameter (Fig. 1c). Time-resolved spectroscopy is a powerful tool for extracting time-multiplexed optical information. Time-resolved CPL has been studied for more than three decades.[3] Recent remarkable progress in CPL spectroscopy has enabled the detection of time-dependent CPL spectral changes on a timescale of less than a nanosecond.[4] Such rapid CPL detection is accomplished using a simple quarter-wave plate instead of a photoelastic modulator (PEM) being capable of directly detecting small differences between LH- and RH-CP light intensities. Consequently, most research in this field has been conducted using a few CP light sources that produce high-intensity light with a high degree of polarization, such as chiral Eu(III) complexes. Therefore, CP light-generating materials for multiplexing optical information require certain capabilities. They must be capable of generating high-intensity light with a high degree of circular polarization, and must have high levels of wavelength and PL lifetime tunability. However, a systematic approach that satisfies all the requirements described above has not yet been reported.

We have previously reported that high-intensity CP light with a high degree of polarization can be generated by a luminescence-based CP convertor comprising a linearly polarized luminescence (LPL) film and a quarter-wave retardation film.[5] The key to this approach is the use of LPL. The intensity, spectral pattern, and polarization degree of the CP light can be tuned by selecting the appropriate LPL materials. The degree of linear polarization ($P_{\text{LP-lum}}$) depends on the orientation of the electronic transition dipole moment in the LPL material, and it
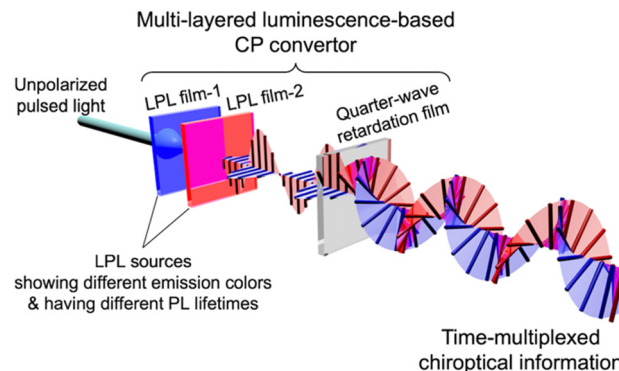
behaves completely independently of the PL quantum yield (ϕ). Therefore, in theory both high ϕ and high $P_{\text{LP-lum}}$ values can be achieved by the selection of an appropriate luminogen and correct orientation of the dipole moment in the LPL material, in contrast to circularly polarized luminescence (CPL), which exhibits a trade-off correlation of these values.[6] LPL with a high $P_{\text{LP-lum}}$ value can be directly converted to CP light while retaining a large degree of polarization. It is possible to determine the sign of the CP light (LH or RH) by selecting the angle ($-45°$ or $+45°$, respectively) between the polarization plane of the LPL film and the fast axis of the quarter-wave retardation film. Furthermore, various types of optical information represented by PL intensity, peak position, polarization, and lifetime can be systematically multiplexed by laminating various LPL films with different optical properties.

Herein, we introduce a novel approach to time-multiplexing chiroptical information using multi-layered luminescence-based CP convertors comprising two LPL films with different PL spectral profiles and PL lifetimes (Fig. 2). The generated time-multiplexed chiroptical information is extracted by time-resolved spectroscopy with classical CP detection (see the ESI†). In the present paper, we demonstrate the generation of time-varying spectral profiles of LH- and RH-CP light and its read-out as temporal chiroptical information.

Results and discussion

In the present study, we selected poly[2-methoxy-5-(2-ethylhexyloxy)-1,4-phenylenevinylene] (MEH-PPV, Fig. 3a) and a CdSe/CdS core/shell quantum rod (QR, Fig. 3b) as luminogens with different PL lifetimes. Because these luminogens have PL spectra with similar emission ranges (approximately 550–700 nm), it is difficult to distinguish each spectral pattern without time resolution. Therefore, we intentionally selected the luminogens to verify the effect of PL lifetime on the spectral pattern. The QR was synthesized by the procedure described in our previous paper.[7] We used poly(ethylene-co-vinyl acetate) (EVA) as a transparent and stretchable polymer media at room temperature. After mixing the luminogen with EVA in toluene, we cast the mixture on a substrate and dried it in air to obtain a
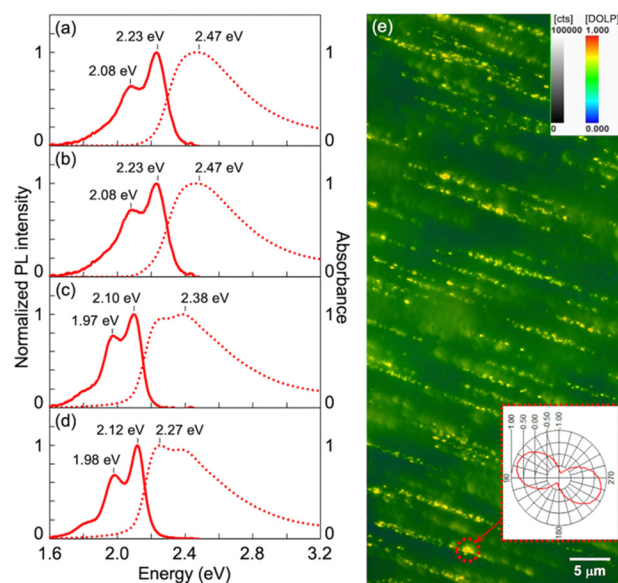
Fig. 3 (a) Chemical structure of MEH-PPV. (b) TEM image of the QRs. Photographs of (c) the LPL$_{MEH-PPV}$ film and (d) the LPL$_{QR}$ film obtained in visible light (left), in UV light (365 nm; middle), and in UV light (365 nm) through a linear polarizer placed parallel ($\parallel$) or perpendicular ($\perp$) to the direction of stretching (right). (e) Absorption (dotted lines) and PL (solid lines) spectra produced by the LPL$_{MEH-PPV}$ film (top) and the LPL$_{QR}$ film (bottom). The red and blue lines indicate parallel ($\parallel$) and perpendicular ($\perp$) LP light components against the stretching direction, respectively. The LPL films were excited with depolarized stationary light at 470 nm. (f) PL lifetime decay curve of the LPL$_{MEH-PPV}$ film (top) and the LPL$_{QR}$ film (bottom). The red dots, red lines, and grey line indicate the recorded data, the fitting curve, and the instrumental response function (IRF), respectively. The LPL films were excited with pulsed light at 470 nm.

luminogen/EVA composite film. We then pealed the resulting film from the substrate, stretched it in one direction, and adhered it to a cover glass. As shown in Fig. 3c and d, both the MEH-PPV/EVA (LPL$_{MEH-PPV}$) and QR/EVA (LPL$_{QR}$) stretched films exhibited good transparency in visible light and strong PL intensity in UV light. There was a marked contrast in light intensity when PL was observed with the naked eye through a linear polarizer placed parallel ($\parallel$) or perpendicular ($\perp$) to the direction of stretching (photographs on the right in Fig. 3c and d). This indicates that both 1D stretched films exhibited LPL with a high degree of polarization. We quantitatively analysed the LPL properties of both the LPL$_{MEH-PPV}$ and LPL$_{QR}$ films by PL spectroscopy with an LP light-detecting setup (see the ESI†). The LPL$_{MEH-PPV}$ and LPL$_{QR}$ films produced strong PL peaks (λ_{max}) at 586 and 605 nm, respectively (Fig. 3e). The degree of linear polarization of the PL (P_{LP-lum}) was calculated using the following equation:

$$P_{LP} = \frac{I_{\parallel} - I_{\perp}}{I_{\parallel} + I_{\perp}} \tag{1}$$

where $I_{\parallel}$ and $I_{\perp}$ are the PL intensities of the parallel and perpendicular LP light components, respectively, at λ_{max} under depolarized exciting light (470 nm). Since these samples are the solid-state thin films, it is also important to consider non-reciprocal component which can be confirmed by film flipping.[8] When spectral measurements were done by placing opposite face of the LPL films, no significant difference was observed in the LPL spectral patterns and the shape of polar plots by all LPL spectral measurements. These results indicate that non-reciprocal component in these LPL films was negligible enough to the measured LPL properties. LPL$_{MEH-PPV}$ film had an extremely large P_{LP-lum} value (0.88), which was higher than that of the LPL$_{QR}$ film (P_{LP-lum} = 0.68). To determine the origin of the large P_{LP-lum} of the LPL$_{MEH-PPV}$ film, we investigated the behavior of MEH-PPV in the LPL$_{MEH-PPV}$ film by absorption and PL spectroscopy. It is well known that MEH-PPV exists as two morphologically distinct species depending on variables such as solvents, concentration, and temperature.[9] One species produces PL from a higher energy state (called the "blue phase") and the other produces PL from a lower energy state (called the "red phase"); the states differ in the extent of delocalization of π-bond electrons.[9a] Fig. 4 compares absorption and PL spectra of MEH-PPV in different environments. An MEH-PPV/toluene solution produced a broaden absorption peak at 2.47 eV (502 nm) and PL peaks at 2.23 eV (556 nm) and 2.08 eV (596 nm), corresponding to the blue phase in which the MEH-PPV polymer chain comprises a disordered coil (Fig. S4a, ESI†). An MEH-PPV/EVA/toluene solution produced similar

Fig. 4 Absorption (dotted lines) and PL (solid lines) spectra of (a) an MEH-PPV/toluene solution, (b) an MEH-PPV/EVA/toluene solution, (c) an MEH-PPV/EVA composite film, and (d) an LPL$_{MEH-PPV}$ film. (e) Degree of linear polarization (DOLP) image of an LPL$_{MEH-PPV/EVA}$ composite film obtained by QROM methodology (Section S1.8 in the ESI†).[10] MEH-PPV/EVA ratio = 2.5×10^{-7} in mass, $\lambda_{excitation}$ = 490 nm, $I_{excitation}$ = 765 μW, $\lambda_{detection}$ > 520 nm. Inset polar plot describes the angular dependence of linear polarization corresponding to the bright area in the red dotted circle.

absorption and PL spectra (Fig. 4b). However, when the MEH-PPV/EVA/toluene solution was dried on a glass substrate to form an MEH-PPV/EVA composite film, both the absorption and PL spectra changed markedly (Fig. 4c). Neither the absorption nor the PL peaks matched those of pure blue and red phases,[9b] indicating the coexistence of blue and red phases without the application of any external force for elongation of the MEH-PPV polymer chain. This phenomenon suggests the formation of MEH-PPV aggregates during the drying process. After stretching the composite film to form an LPL$_{MEH-PPV}$ film, we observed similar absorption and PL spectra with a slight sharpening of the PL peaks (Fig. 4d). Such vibrationally resolved peaks can be explained by the increasing local rigidity of MEH-PPV polymer chain. These results indicate that the MEH-PPV polymer chain align in one direction and the stacking of MEH-PPV polymer chain was enhanced (Fig. S2, ESI†). The fluorescence polarization microscopy results supported this idea. As shown in Fig. 4e, we observed highly emissive domains in the LPL$_{MEH-PPV}$ film, each with a high degree of polarization and aligned along the stretching direction, whereas we observed homogeneous emission everywhere in the LPL$_{QR}$ film (Fig. S3, ESI†). These results indicate that the bundle-shaped highly emissive domains originated from the phase separation of MEH-PPV from the EVA matrix at the microscopic level, and contributed significantly to the large P_{LP-lum} value of the LPL$_{MEH-PPV}$ film, in contrast to the homogeneously suspended QRs in the EVA matrix. We fabricated a series of multi-layered luminescence-based CP convertors to investigate the multiplexing of chiroptical information. Each convertor was produced by laminating an LPL$_{MEH-PPV}$ film and an LPL$_{QR}$ film on a quarter-wave film. We varied the angle between the polarization axes of the LPL films and the fast axis of the quarter-wave film. The angles between the polarization axes of the LPL$_{MEH-PPV}$ ($\theta_{MEH-PPV}$) and LPL$_{QR}$ (θ_{QR}) films and the fast axes of the quarter-wave retardation films can be summarized as follows: $\theta_{MEH-PPV} = \theta_{QR} = -45°$ (Multi-V$_{MEH-PPV}$V$_{QR}$; Fig. 5a); $\theta_{MEH-PPV} = -45°$ and $\theta_{QR} = +45°$ (Multi-V$_{MEH-PPV}$H$_{QR}$; Fig. 5c); $\theta_{MEH-PPV} = +45°$ and $\theta_{QR} = -45°$ (Multi-H$_{MEH-PPV}$V$_{QR}$; Fig. 5e); and $\theta_{MEH-PPV} = \theta_{QR} = +45°$ (Multi-H$_{MEH-PPV}$H$_{QR}$; Fig. 5g). Fig. 5 shows the $2 \times 2 = 4$ different CP convertors and each LH- and RH-CP light spectral profile. When the PL spectra were obtained without using a polarization setup, we did not detect any significant differences between the four types of CP convertors (black dotted lines in Fig. 5b, d, f, and h). However, we obtained four distinctly different sets of chiroptical information (red and blue solid lines in Fig. 5b, d, f, and h). These results indicate that chiroptical information can be easily tuned while retaining the PL spectral pattern and PL intensity by changing the angle between the polarization axes of the LPL films and the fast axis of the quarter-wave retardation film. Note that even Multi-V$_{MEH-PPV}$V$_{QR}$ (or Multi-H$_{MEH-PPV}$H$_{QR}$) had an RH-CP (or LH-CP) component. That was because both P_{LP-lum} values were less than 1, *i.e.*, the light generated from both LPL films always contained a small perpendicular PL component, which resulted in the production of an opposite-handed CP light component. The production of
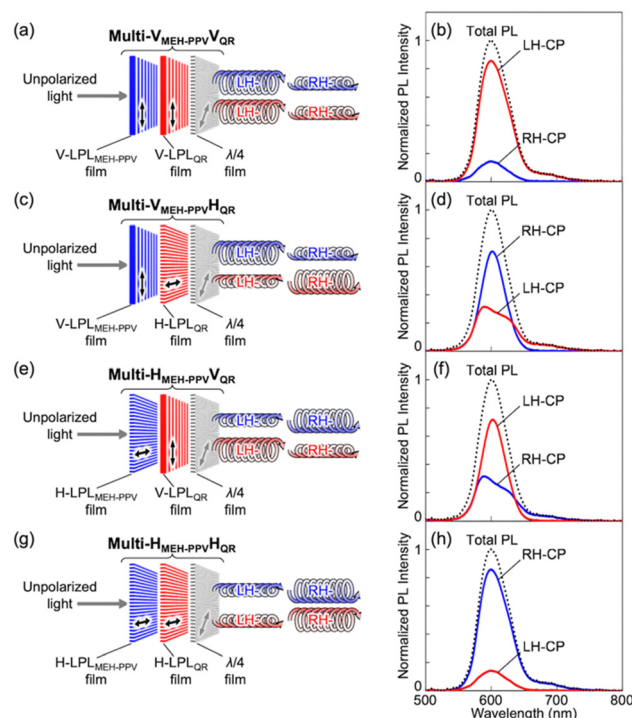

Fig. 5 Schematic illustration of (a) Multi-V$_{MEH-PPV}$V$_{QR}$, (c) Multi-V$_{MEH-PPV}$H$_{QR}$, (e) Multi-H$_{MEH-PPV}$V$_{QR}$, and (g) Multi-H$_{MEH-PPV}$H$_{QR}$. PL spectra of (b) Multi-V$_{MEH-PPV}$V$_{QR}$, (d) Multi-V$_{MEH-PPV}$H$_{QR}$, (f) Multi-H$_{MEH-PPV}$V$_{QR}$, and (h) Multi-H$_{MEH-PPV}$H$_{QR}$ excited by depolarized light at 470 nm. The red and blue lines indicate LH- and RH-CP light components, respectively. The black dotted lines indicate total PL intensity. The total PL values were normalized so that the highest peak equalled one.

opposite-handed CP light components was also observed in Multi-V$_{MEH-PPV}$H$_{QR}$ and Multi-H$_{MEH-PPV}$V$_{QR}$. This proved that the P_{LP-lum} values (0.68 and 0.88) were high enough to produce multiplexed chiroptical information, which it was possible to detect using a classical CP detection setup. Polarization degree of CP light (P_{CP}) was calculated by the following equation:

$$P_{CP} = \frac{I_{LH} - I_{RH}}{I_{LH} + I_{RH}} \tag{2}$$

where I_{LH} and I_{RH} are the intensities of LH- and RH-CP light components, respectively. When CP light is produced by CPL, dissymmetry factor (g), which is calculated by the following equation, is commonly used to quantitatively evaluate the degree of CP.

$$g = \frac{2(I_{LH} - I_{RH})}{I_{LH} + I_{RH}} \tag{3}$$

Since photoluminescence phenomenon in luminescence-based CP convertor is not CPL but LPL, to be precise, g value should not be used for evaluating polarization degree of CP light. However, we dare to show each g value in Fig. S4–S6 (ESI†) for a simple comparison of their performance with many other CPL systems. The Multi-V$_{MEH-PPV}$V$_{QR}$ and Multi-H$_{MEH-PPV}$H$_{QR}$ showed large P_{CP} values (0.72 and −0.72) corresponding to values between that of single-layered CP convertors (Fig. S4 and S5, ESI†). In the case of Multi-V$_{MEH-PPV}$H$_{QR}$, relatively smaller
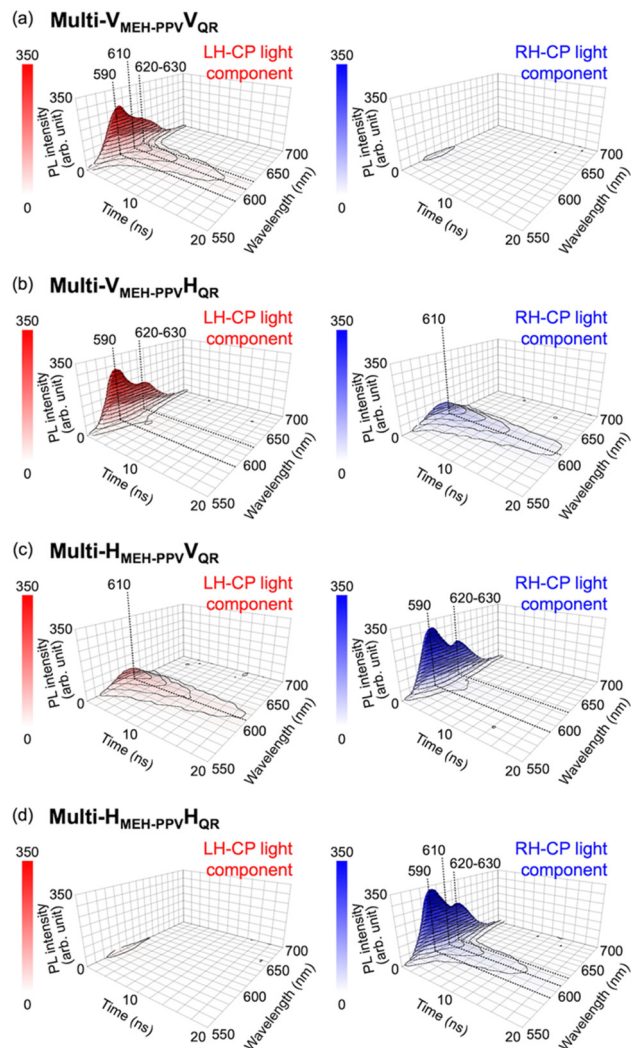
Fig. 6 Time-course changes in LH- (left) and RH- (right) CP light generated by (a) Multi-$V_{MEH\text{-}PPV}V_{QR}$, (b) Multi-$V_{MEH\text{-}PPV}H_{QR}$, (c) Multi-$H_{MEH\text{-}PPV}V_{QR}$, and (d) Multi-$H_{MEH\text{-}PPV}H_{QR}$. Red and blue indicate the light intensities of the LH- and RH-CP components, respectively. Each convertor was excited by depolarized pulsed light at 470 nm.

Fig. 7 (a) Time-course changes in PL spectra of Multi-$V_{MEH\text{-}PPV}V_{QR}$, Multi-$V_{MEH\text{-}PPV}H_{QR}$, Multi-$H_{MEH\text{-}PPV}V_{QR}$, and Multi-$V_{MEH\text{-}PPV}H_{QR}$. The total PL values were normalized so that the highest peak equalled one. The red and blue lines indicate LH- and RH-CP components, respectively. The black dotted lines indicate the total PL. Each convertor was excited by depolarized pulsed light at 470 nm. (b) Time-course changes in PL intensity of LH-CP components at 590 nm (blue lines in the two graphs on the left) and RH-CP components at 610 nm (red lines in the two graphs on the left) produced by Multi-$V_{MEH\text{-}PPV}V_{QR}$ and Multi-$V_{MEH\text{-}PPV}H_{QR}$. Time-course changes in PL intensity of LH-CP components at 610 nm (red lines in the two graphs on the right) and RH-CP components at 590 nm (blue lines in the two graphs on the right) produced by Multi-$H_{MEH\text{-}PPV}V_{QR}$ and Multi-$H_{MEH\text{-}PPV}H_{QR}$.

P_{CP} value with negative sign (−0.43) was observed at about 600 nm, where the emission from $LPL_{MEH\text{-}PPV}$ and LPL_{QR} films were overlapped (Fig. S6b, ESI†). Whereas large P_{CP} value with positive sign (0.8–0.9) was observed in the non-overlapped wavelength region above 660 nm. Similar result with opposite sign was observed in Multi-$H_{MEH\text{-}PPV}V_{QR}$ (Fig. S6c, ESI†).

Because each of the four types of multi-layered luminescence-based CP convertors (Multi-$V_{MEH\text{-}PPV}V_{QR}$, Multi-$V_{MEH\text{-}PPV}H_{QR}$, Multi-$H_{MEH\text{-}PPV}V_{QR}$, and Multi-$H_{MEH\text{-}PPV}H_{QR}$) comprised two LPL films with different PL lifetimes, the generated CP light was considered to include temporal information. We obtained time-resolved spectral measurements using a fluorescence lifetime spectrometer operated with a CP light detection setup to evaluate the time-multiplexing of the chiroptical information generated by each convertor (see ESI†). As shown in Fig. 6, the PL spectral profiles of both the LH- and RH-CP components changed markedly over time. The time-course
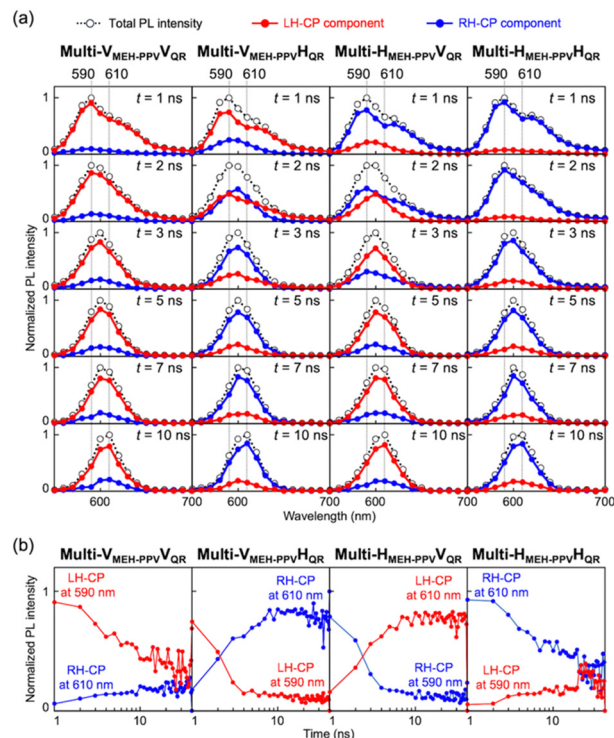
changes of the LH-CP component from Multi-$V_{MEH\text{-}PPV}V_{QR}$ exhibited rapid attenuation of the double peak (590 nm and 620–630 nm), and slow attenuation of the single peak (610 nm) (Fig. 6a, left). The former and the latter signals can be attributed to emissions from MEH-PPV and QR, respectively. A similar result was observed for the RH-CP component from Multi-$H_{MEH\text{-}PPV}H_{QR}$ (Fig. 6d, right). In the case of Multi-$V_{MEH\text{-}PPV}H_{QR}$ (or Multi-$H_{MEH\text{-}PPV}V_{QR}$), the emission exhibited two different attenuation behaviors clearly separated into two CP light components with opposite handedness (Fig. 6b and c). Fig. 7a shows the spectral profiles of the total PL, LH-CP, and RH-CP components in the first 10 ns. All the initial spectral patterns of the total PL from the four convertors changed markedly within 10 ns and exhibited a peak shift from 590 to 610 nm (black empty circles and dotted lines in Fig. 7a). The changes in the LH- and RH-CP light profiles of Multi-$V_{MEH\text{-}PPV}V_{QR}$ and Multi-$H_{MEH\text{-}PPV}H_{QR}$ were similar to that of the total PL. However, the main components in the light generated by Multi-$V_{MEH\text{-}PPV}H_{QR}$ and Multi-$H_{MEH\text{-}PPV}V_{QR}$ switched within 3 ns, as shown in Fig. 7b. These results indicate that it is

possible to generate time-multiplexed chiroptical information from the multilayer-type luminescence-based CP convertor by simply selecting the appropriate LPL films and azimuthal $\theta_{\text{luminogen}}$ angles.

Conclusions

Herein, we reported the first example of time-multiplexing chiroptical information using a multilayer-type luminescence-based circular polarization convertor comprising two LPL films with different PL spectral profiles and different PL lifetimes. We fabricated LPL films with short and long PL lifetimes by uniaxial stretching MEH-PPV/EVA and QR/EVA composite films, respectively. The large polarization degree of the LPL ($P_{\text{LP-lum}} = 0.88$) was attributable to the LPL$_{\text{MEH-PPV}}$ film, which contained bundle-shaped highly emissive domains. Using both LPL$_{\text{MEH-PPV}}$ and LPL$_{\text{QR}}$ films, we fabricated four different multilayer-type luminescence-based CP convertors by selecting the azimuthal angles between the polarization axes of the LPL films and the fast axes of the quarter-wave films. The prepared CP convertors generated four different types of steady-state chiroptical information. Time-varying of CP light spectral profiles were successfully produced by the four CP convertors and was extracted as time-multiplexed chiroptical information by time-resolved spectroscopy with CP detection. These findings will enable the design of novel CP light-generating materials for various fields, including time-multiplexed anti-counterfeit printing and optical data storage systems.

Author contributions

Y. Okazaki designed the project, raised funds, and wrote the original draft. M. Kimura prepared the LPL$_{\text{QR}}$ film. K. Nakamura prepared the LPL$_{\text{MEH-PPV}}$ film. H. Shimizu prepared all the multi-layered luminescence-based CP convertors. All the experimental measurements, observations, and analyses were carried out by Y. Okazaki and H. Shimizu, who made equal contributions. The fluorescence polarization microscopy study was carried out by G. Raffy and A. Del Guerzo. The time-resolved spectral measurements were supported by K. Yoshida and M. Takafuji. All the authors discussed the results and contributed to the interpretation of the data.

Conflicts of interest

There are no conflicts to declare.

Acknowledgements

Notes and references

1 (a) S. Lin, Y. Tang, W. Kang, H. K. Bisoyi, J. Guo and Q. Li, *Nat. Commun.*, 2023, **14**, 3005; (b) X. Yu, D. Zhang, M. Xu, G. Song and Y. Xu, *J. Mater. Chem. C*, 2023, **11**, 1684–1689; (c) Y. Shi, J. Han, X. Jin, W. Miao, Y. Zhang and P. Duan, *Adv. Sci.*, 2020, **9**, 2201565; (d) M. Kim, H. Lee, R. T. Snipes, M. J. Han and V. V. Tsukruk, *Small*, 2022, **18**, 2104340; (e) H. Li, H. Li, W. Wang, Y. Tao, S. Wang, Q. Yang, Y. Jiang, C. Zheng, W. Huang and R. Chen, *Angew. Chem., Int. Ed.*, 2020, **59**, 4756–4762; (f) S. Ito, K. Ikeda, S. Nakanishi, Y. Imai and M. Asami, *Chem. Commun.*, 2017, **53**, 6323–6326.

2 (a) E. M. Sánchez-Carnerero, A. R. Agarrabeitia, F. Moreno, B. L. Maroto, G. Muller, M. J. Ortiz and S. de la Moya, *Chem. – Eur. J.*, 2015, **21**, 13488–13500; (b) J. Kumar, T. Nakashima and T. Kawai, *J. Phys. Chem. Lett.*, 2015, **6**, 3445–3452; (c) Y. Sang, J. Han, T. Zhao, P. Duan and M. Liu, *Adv. Mater.*, 2020, **32**, 1900110; (d) G. Albano, G. Pescitelli and L. Di Bari, *Chem. Rev.*, 2020, **120**, 10145–10243; (e) S. Jiang and N. A. Kotov, *Adv. Mater.*, 2022, 2108431.

3 (a) J. Ferguson and E. R. Krausz, *Chem. Phys. Lett.*, 1982, **93**, 21–25; (b) D. H. Metcalf, S. W. Snyder, S. Wu, G. L. Hilmes, J. P. Riehl, J. N. Demas and F. S. Richardson, *J. Am. Chem. Soc.*, 1989, **111**, 3082–3083; (c) D. H. Metcalf, S. W. Snyder, J. N. Demas and F. S. Richardson, *J. Am. Chem. Soc.*, 1990, **112**, 469–479; (d) M. F. Reid, *J. Lumin.*, 1990, **45**, 384–386; (e) D. H. Metcalf, S. W. Snyder, J. N. Demas and F. S. Richardson, *J. Phys. Chem.*, 1990, **94**, 7143–7153; (f) P. M. L. Block, P. Schakel and H. P. J. M. Dekkers, *Meas. Sci. Technol.*, 1990, **1**, 126–130; (g) L. Geng and L. B. McGown, *Anal. Chem.*, 1992, **64**, 68–74; (h) J. A. Schauerte, D. G. Steel and A. Gafni, *Proc. Natl. Acad. Sci. U. S. A.*, 1992, **89**, 10154–10158.

4 (a) D. F. De Rosa, P. Stachelek, D. J. Black and R. Pal, *Nat. Commun.*, 2023, **14**, 1537; (b) B. Baguenard, A. Bensalah-Ledoux, L. Guy, F. Riobé, O. Maury and S. Guy, *Nat. Commun.*, 2023, **14**, 1065; (c) U. Hananel, G. Schwaartz, G. Paiss, L. Arrico, F. Zinna, L. Di Bari, O. Cheshnovsky and G. Markovich, *Chirality*, 2021, **33**, 124–133; (d) L. E. MacKenzie, L.-O. Pålsson, D. Parker, A. Beeby and R. Pal, *Nat. Commun.*, 2020, **11**, 1676; (e) S. A. Bourelle, R. Shivanna, F. V. A. Camargo, S. Ghosh, A. J. Gillett, S. P. Senanayak, S. Feldmann, L. Eyre, A. Ashoka, T. W. J. van de Goor, H. Abolins, T. Winkler, G. Cerullo, R. H. Friend and F. Deshler, *Nano Lett.*, 2020, **20**, 5678–5685; (f) A. T. Frawley, R. Pal and D. Parker, *Chem. Commun.*, 2016, **52**, 13349–13352.

5 Y. Okazaki, M. Kimura, K. Hachiya and T. Sagawa, *J. Mater. Chem. C*, 2023, **11**, 935–942.

6 (a) P. M. L. Block and H. P. J. M. Dekkers, *Chem. Phys. Lett.*, 1989, **161**, 188–194; (b) Y. Nagata and T. Mori, *Front. Chem.*, 2020, **8**, 448; (c) L. Arrico, L. Di Bari and F. Zinna, *Chem. – Eur. J.*, 2021, **27**, 2920–2934.

7 (a) L. Carbone, C. Nobile, M. De Giorgi, F. D. Sala, G. Morello, P. Pompa, M. Hytch, E. Snoeck, A. Fiore, I. R. Franchini, M. Nadasan, A. F. Silvestre, L. Chiodo, S. Kudera, R. Cingolani, R. Krahne and L. Manna, *Nano Lett.*, 2007, **7**, 2942–2950; (b) J. Dehnel, Y. Barak, I. Meir, A. K. Budniak, A. P. Nagvenkar, D. R. Gamelin and E. Lifshitz, *ACS Nano*, 2020, **14**, 13478–13490.

8 G. Albano, G. Pescitelli and L. Di Bari, *ChemNanoMat*, 2022, **8**, e202200219.

9 (a) A. Köhler, S. T. Hoffmann and H. Bässler, *J. Am. Chem. Soc.*, 2012, **134**, 11594–11601; (b) F. C. Spano and C. Silva, *Annu. Rev. Phys. Chem.*, 2014, **65**, 477–500.

10 A. Chakrabarty, G. Raffy, M. Maity, L. Gartzia-Rivero, S. Marre, C. Aymonier, U. Maitra and A. Del Guerzo, *Small*, 2018, **14**, 1802311.